Microchimica Acta (2019) 186: 252
https://doi.org/10.1007/s00604-019-3349-1

ORIGINAL PAPER

An integrated magnetic microfluidic chip for rapid immunodetection of the prostate specific antigen using immunomagnetic beads

Zhu Feng[1] · Shaotao Zhi[1] · Lei Guo[1] · Yong Zhou[1] · Chong Lei[1]

Received: 23 January 2019 / Accepted: 27 February 2019 / Published online: 22 March 2019

Abstract

The authors describe an integrated microfluidic chip for immunodetection of the prostate specific antigen (PSA) by using giant magnetoimpedance (GMI) sensor. This chip contains an immunoreaction platform and a biomarker detection system. The immunoreaction platform contains an incubation chamber and a reactive chamber to implement immunological reaction in microfluidics. The system can detect PSA rapidly with ultra-high sensitivity. Both are fabricated by MEMS technology. Immunomagnetic beads (If PSA binds to its antibody (that is labeled with immunomagnetic beads; IMBs) it will be trapped on the surface of self-assembled film. Trapped IMBs generate a stray magnetic field under the magnetization of the external applied magnetic field and can be detected by the GMI sensor. The chip can detect PSA with a detection limit as low as 0.1 ng · mL^{-1} and works in the 0.1 ng · mL^{-1} to 20 ng · mL^{-1} concentration range. Compared to established GMI biosensors, the magnetic microfluidic chip reduces assay time, and lends itself to fast detection. It also avoids complex handling steps, enhances reaction efficiency and decreases experimental errors.

Keywords Prostate specific antigen · Microfluidic chip · Point-of-care diagnostics · Giant magnetoimpedance · Micro-electromechanical systems · Immunomagnetic beads · Immunoreaction platform · Biomarker detection · Magnetic sensor · Biosensor

Introduction

Prostate cancer (PCa) has become the second most common cause of cancer and is the sixth leading cause of death by cancer for male in the worldwide [1]. Diagnosis and prognosis of PCa are in increasing demands and require the development of detecting PCa-related biomarkers sensitively and accurately. Prostate specific antigen (PSA) is the most reliable tumor biomarker in the early clinical diagnosis and subsequent treatment of PCa [2]. In healthy males, the concentration of PSA in serum samples is in the range of 1 − 4 ng · mL^{-1}. For a PSA level of 4 − 10 ng · mL^{-1}, there exists a 22 − 27% likelihood of developing PCa, while for values above 10 ng · mL^{-1}, the risk increases to 67% [3].

Many sensitive quantitative detection techniques, for instance, Enzyme Linked Immunosorbent Assay (ELISA) [4, 5], electrochemical immunoassay [6] and bioluminescent immunoassay [7], have been widely conducted on clinical sample measurements. In recent years, micro-magnetic sensors have been applied into biosensing chips for the advantages of low background signal, fast response speed, environmental friendly and high flexibility [8]. Comparing with other micro-magnetic sensors (e.g., giant magnetoresistance (GMR) based sensors [8, 9], micro-hall sensors [10] and micro-fluxgate sensors [11]), giant magnetoimpedance (GMI) based sensors have the property of ultra-high sensitivity and high detection threshold [12, 13]. So GMI sensors have attracted much attention of their potential application in biomarker detection [14]. Up to now, GMI biosensors are mainly fabricated by soft amorphous ferromagnetic ribbons [15] and thin films [14, 16]. GMI biosensors fabricated by

✉ Zhu Feng
feng.z@sjtu.edu.cn

✉ Chong Lei
leiqhd@sjtu.edu.cn

[1] Key Laboratory of Thin Film and Microfabrication (Ministry of Education), Department of Micro-Nano Electronics, School of Electronic Information and Electrical Engineering, Shanghai Jiao Tong University, Dongchuan Road 800, Shanghai 200240, China

ribbons have the advantages of brief steps and compatible with biochip in microfabrication process, capable of integrating with immunoreaction platform as well as excellent magnetic performance.

Immunomagnetic beads (IMB) process excellent superparamagnetic properties and biocompatibility [16, 17], which are used as magnetic labels in biomarker detection. Utilizing magnetic biosensors to detect IMB labeled biomarkers has generated considerable research interest. One advantage of IMB is the low background noise in immunoreaction because all other components are essentially non-magnetic. In addition, IMB induce stray field under the magnetization of external DC magnetic field and can be detected by magnetic sensor. As a result, IMB are well applied to magnetic biosensing chip. For high effective immunoreaction of PSA before magnetic detection, PSA labeled by IMB can be immobilized on the surface of self-assembled Au film by double antibody sandwich immunoassay and streptavidin-biotin binding assay. In biomarker detection system, IMB were employed as magnetic labels to generate stray magnetic field and the variation of magnetic signal was detected by GMI sensor.

Point-of-care (PoC) diagnostics which have the characteristics of disposability, cost-effectiveness, ease of use and portability, offer great potential to detect and monitor diseases at resource-limited settings [18]. Up to now, a few biomarkers have been detected by traditional GMI biosensing systems [14, 19, 20], however, these systems are hard to be adapted for PoC testing for the following factors. First, traditional detection methods have a complex series of steps in immunoassay, so they require complicated operations and are difficult to reach integration in one chip. Second, owing to solutions are dropwise added on the reaction Au film, the distributions of IMB labeled biomarkers on Au film are prone to vary between laboratories and produce different magnetic signals in different experiments. Thus, it is difficult to achieve reproducibility in experiment, particularly at low biomarker concentrations. Third, it is hard to identify the position relationship between immunoreaction platform and GMI sensor accurately in separable detection. Therefore, experiment errors caused by the inaccurate position relationship in magnetic signal test are increased. Based on the discussion above, an integrated magnetic microfluidic chip requires to be designed and fabricated to satisfy PoC testing rapidly.

Microfluidics offers the advantages such as analyzing biomarkers accurately and efficiently, small and constant volume, short assay time, as well as test platform integrated [21, 22]. Microfluidics-based analysis system is well positioned to contribute in detecting various biomarkers conveniently and holds promise for further PoC diagnosis. To accomplish PSA immunodetection rapidly, immunoreaction, IMB labeled PSA trapping and magnetic signal testing processes are implemented in a microfluidics-based analysis chip.

In our work, an integrated magnetic microfluidic chip was designed and microfabricated by MEMS technology. This chip contains an immunoreaction platform and a biomarker detection system. The chip can detect PSA rapidly, and has promise in PoC diagnostic applications. In order to implement immunological reaction in microfluidics, the immunoreaction platform contains incubation chamber and reactive chamber. The immunodetection is implemented in microfluidics: PSA is conjugated with IMB labeled PSA antibody and is trapped on the surface of self-assembled Au film. Trapped IMB generate stray magnetic field under the magnetization of the external applied DC magnetic field. The change of impedance induced by IMB is detected by GMI sensor in biomarker detecting system. To the best of authors' acknowledge, this report describes the first demonstration of a microfluidic chip using a GMI sensor to detect biomarker.

Methods

Materials and reagents

Photoresist was supplied by AZ Electronic Material Ltd. (Suzhou, China, https://suzhou0260244.3566t.com/). SU-8 negative photoresist was purchased from Micro Chem (Westborough, USA, http://microchem.com/). Polydimethylsiloxane (PDMS, Sylgard 184) was purchased from Dow Corning (Michigan, USA, https://consumer.dow.com/). Polyimide was supplied by Beijing POME Technology Co. Ltd. (Beijing, China, http://www.pome.com.cn/).

Hydrochloricacid (HCl), acetone and hydrogen peroxide (H_2O_2) were sourced from Sinopharm Chemical Reagent (Shanghai, China, https://www.reagent.com.cn/). Nitric Acid (HNO_3) was purchased from Lingfeng Chemical Reagent Co. Ltd. (Shanghai, China, http://www.yonghuachem.com/). Ethanol was purchased from Shanghai Titan Scientific Co. Ltd. (Shanghai, China, http://www.titansci.com/). Sodium hydroxide (NaOH) was supplied by Pinghu Chemical Reagent (Pinghu, China, http://phhg.nbchem.com/).

Human PSA, mouse PSA antibody and biotinylated mouse PSA antibody were purchased from Linc-Bio Science Co. Ltd. (Shanghai, China, http://www.linc-bio.cn/). Dynabeads® Myone™ streptavidin M-280 and DynaMag™-Spin Magnet were purchased from ThermoFisher Scientfic (Waltham, USA, https://www.thermofisher.com/). 3-Mercaptopropionic acid (MPA) was purchased from Shanghai Titan Scientific Co. Ltd. (Shanghai, China, http://www.titansci.com/). 1-ethyl-3-[3-dimethylaminoprop-yl] carbodiimide (EDC) hydrochloride was purchased from Aladdin Chemistry Co. Ltd. (Beijing, China, http://www.aladdin-e.com/). N-Hydroxysulfosuccinimide sodium salt (NHS) was purchased from Medpep Co. Ltd. (Shanghai, China, http://www.medpep.com/). Albumin from bovine serum (BSA) was purchased from Via-gene pro bio Technologies Co. ltd. (Shanghai,

China, https://www.wegene.com/). Phosphate buffer saline (PBS) and PBS with 0.05% Tween™ 20 tablets were supplied by Medicago AB (Uppsala, Sweden, http://www.medicago.se/). In all experiments, deionized water was used.

Instrumentations

Magnetic-field annealing oven A1241A-JD was purchased from Shanghai Zhen Dong Engineering and Equipment Research Institute (Shanghai, China, http://www.shzhendong.com/). Syringe pump LSP01-1A and LSP02-1B were sourced from Longer Precision Pump Co. Ltd. (Baoding, China, https://www.longerpump.com/). Real-time tracking of biomarkers and magnetic beads was implemented using a VHX-5000 optical microscope with CCD camera and image/video recording system (Osaka, Japan, https://www.keyence.com.cn/). The magnetoimpedance effect was measured by impedance analyzer Hewlett-Packard (HP) 4194A (California, USA, https://www.keysight.com/).

Design and simulation of magnetic trapping array

To rapidly and efficiently manipulate PSA, the integrated magnetic microfluidic chip contains immunoreaction platform and biomarker detection system. The schematic plot of integrated magnetic microfluidic chip is shown in Fig. 1a. In immunoreaction platform, double antibody sandwich immunoassay was employed for PSA immobilization and streptavidin-functioned IMB were binding with biotinylated PSA antibody for labeling as biomarker. Trapping IMB effectively is of great importance to guarantee the efficiency of antigen-antibody reaction.

On the macroscale, immunomagnetic beads (IMBs) which essentially act as magnetic dipoles were acted by magnetic force. Due to the dipole-dipole interaction, IMB tended to form chains oriented along the magnetic field direction . The magnetic force $\overrightarrow{F_{mag}}$ generated from magnetic field was used to manipulate the IMBs, which is given by [23].

$$\overrightarrow{F_{mag}} = \mu_f V\left(\overrightarrow{M_P}\cdot\overrightarrow{\nabla}\right)\overrightarrow{H_a}$$

where μ_f is the permeability of the transport fluid, V and M_P are the mean volume and magnetization of the IMBs, and H_a represents the applied magnetic field excited by magnets. To trap IMBs efficiently, not only strong absolute magnetic field intensity but also large magnetic field gradient is required. Comparing with a strong but uniform permanent magnet, alternately arranged magnets with opposite polarities next to each other make a large magnetic field gradient. According to our work, a large magnetic field gradient is induced by the alternating arrangement of six permanent magnets, as shown in Fig. 1b. The magnetic flux density characteristics of permanent magnet array were simulated by the COMSOL software. Each side length of magnet is 2 mm. Figure 1c displays the magnetic flux density of permanent magnet array.

In addition, magnetic ribbon has the property of high permeability and high saturation induction. Magnetic sensor fabricated by magnetic ribbon can enhance the trapping force of IMBs in the microchannel. Figure 1d plots the simulated magnetic flux density distribution at the bottom of microchannel. Strong magnetic field intensity and large magnetic field gradient are mainly induced by the edges of each magnet in the magnetic array and the edges of magnetic ribbon. Figure 1e displays the simulated magnetic flux density distribution at top (500 μm above the surface) of microchannel. The edges of magnets induce strong magnetic field intensity and the edges of ribbon produce large magnetic field gradient.

Fabrication of the GMI sensor

Biomarker detection system applies Cobalt-based GMI sensor fabricated by MEMS technology in PSA detection. Co-based alloy ribbon with a nominal composition of CoFeSiNiB, has a thickness of 15 μm. Figure 2a displays Scanning Electron Microscope (SEM) characterizations of Co-based ribbon and it can be inferred that the ribbon processes the irregular surface topography. Before GMI sensor fabrication, the ribbon was implemented by magnetic field anneal in magnetic-field annealing oven to release the residual stress and reduce the hysteresis loss. In this way, the performance of soft magnetic material was enhanced.

The GMI sensor was fabricated by standard UV photolithography and wet etching technique, which has been described elsewhere [24]. As shown in Fig. 2b, the meander-line structure GMI sensor consists of 3 turns in serial connection with the strip length 5000 μm, the width 150 μm, and the interval of strips 450 μm.

Design and fabrication of the integrated magnetic microfluidic chip

To integrate immunoreaction platform and biomarker detection system in one magnetic microfluidic chip, Au film was sputtered on the GMI sensor to implement immunoreaction in microfluidics. GMI-based magnetic immunoassay which fabricated by sandwich NiFe/Cu/NiFe film with a meander-line structure has been reported in the detection of biomarkers in situ testing previously [19]. However, as for the living technology and condition, it is hard to fix Au film above the GMI sensor fabricated by soft amorphous ferromagnetic ribbon in a predefined position. In our work, electroplating position marks are first adopted to fix GMI sensor in a certain position. Therefore, the relationship between GMI sensor and Au film is confirmed. This procedure solves the problem of fixing Au

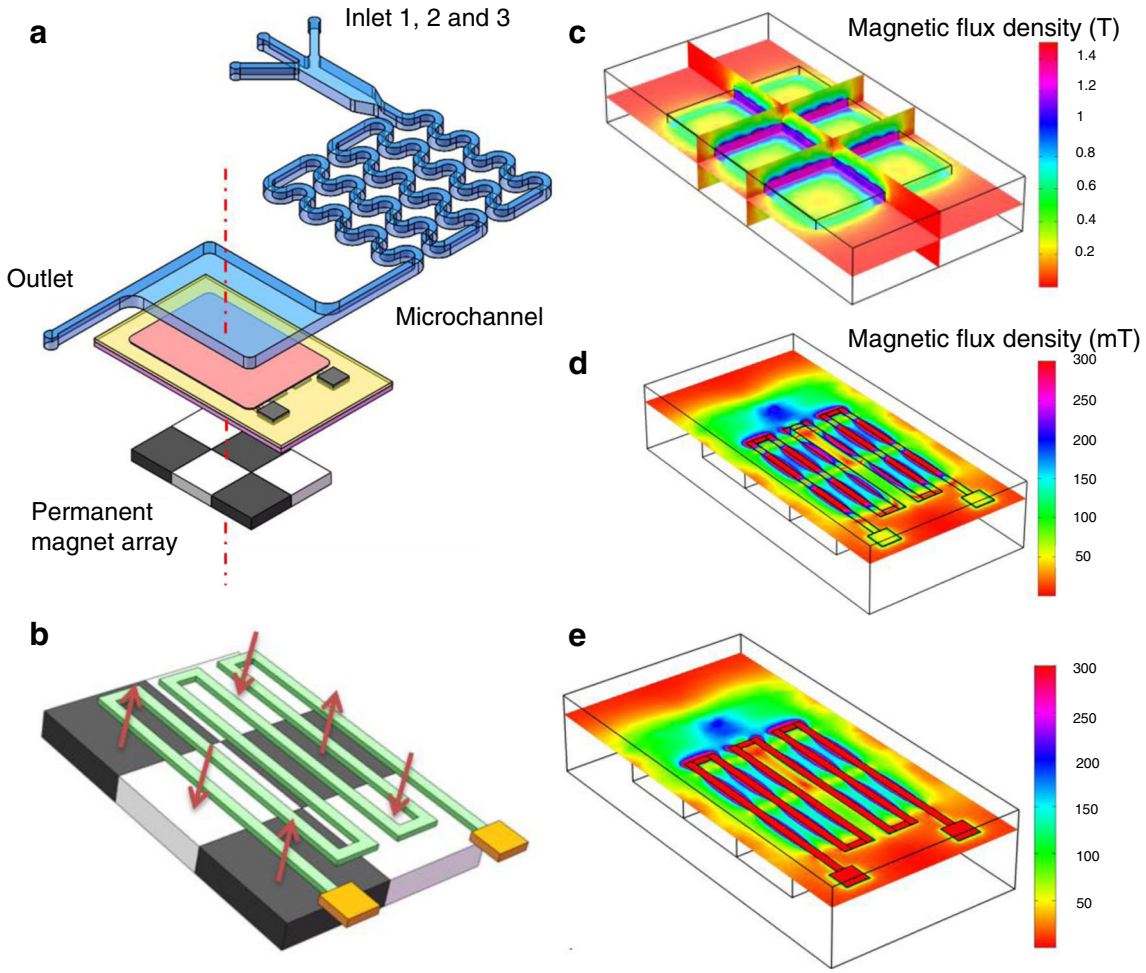

Fig. 1 **a** Schematic plot of integrated magnetic microfluidic chip. **b** Alternating arrangement of six permanent magnets and magnetic ribbon in magnetic trapping array. **c** Magnetic flux density of permanent magnet array. **d** Magnetic flux density distribution at the bottom of the microchannel. **e** Magnetic flux density distribution at the top (500 μm above the surface) of the microchannel

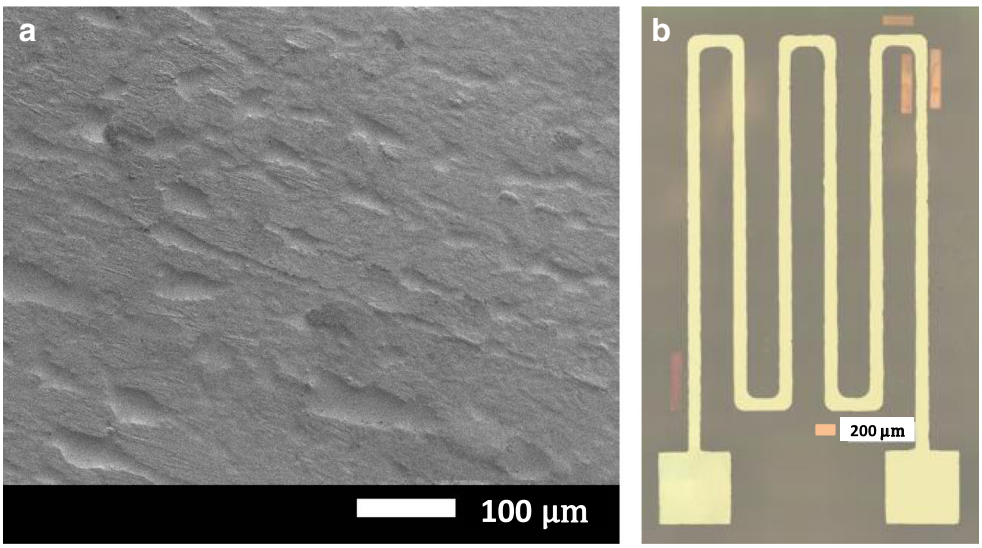

Fig. 2 **a** SEM characterizations of Co-based ribbon. **b** Micrograph of meander-line structure GMI sensor

film on the GMI sensor, increases the fabrication success rate and standardizes process flow.

The biomarker detecting system is fabricated by standard microfabrication technology and Fig. 3 displays fabrication procedure of magnetic microfluidic chip. The detail processes are as follows: To start the fabrication of platform, a 100 nm Cr/Cu seed layer was sputtered on a cleaned glass substrate. A 15 μm photoresist layer was spin-coated onto the seed layer and patterned using exposure and development. Then, copper was electroplated on the seed layer as position marks. Photoresist was removed by acetone and the seed layer was removed by reactive ion etching (RIE) (Step 1). The patterned Co-based GMI sensors were glued on the substrate by thin polyimide and their position was accurately fixed by position marks (Step 2). After solidification in oven, another thin coating of polyimide was spin-coated on the wafer, solidified in oven again and fine polished. Electrodes were microfabricated using the sequence of sputtering seed layer, lithography, electroplating copper, spin-coating polyimide and polish, which is similar to fabrication process of position marks. In particular, polyimide film was served as an isolating layer between GMI sensor and biological reactive solution (Step 3). Au film in reactive chamber was fabricated by lift-off technology: A 5 μm photoresist layer was spin-coated onto the polyimide film and a 200 nm Au/Cr film was sputtered on the photoresist. The total area of Au film is 6 mm × 4 mm. Photoresist was removed by acetone and Au film was remained above GMI ribbon (Step 4).

In order to implement immunological reaction in microfluidics, the platform contains incubation chamber and reactive chamber. Microfluidic channel was microfabricated using the standard molding technique of replicating a PDMS structure from an SU-8 mold. SU-8, a negative photoresist, was spin-coated onto a clean silicon substrate at a thickness of 500 μm after a 2 h bake above 180°C. The substrate was exposed by UV lithography to form the desired pattern through a photomask. Once the mold is complete, PDMS pre-polymer and curing agent were mixed according to 10:1 by weight and PDMS structure was formed by pouring the mixed PDMS on the

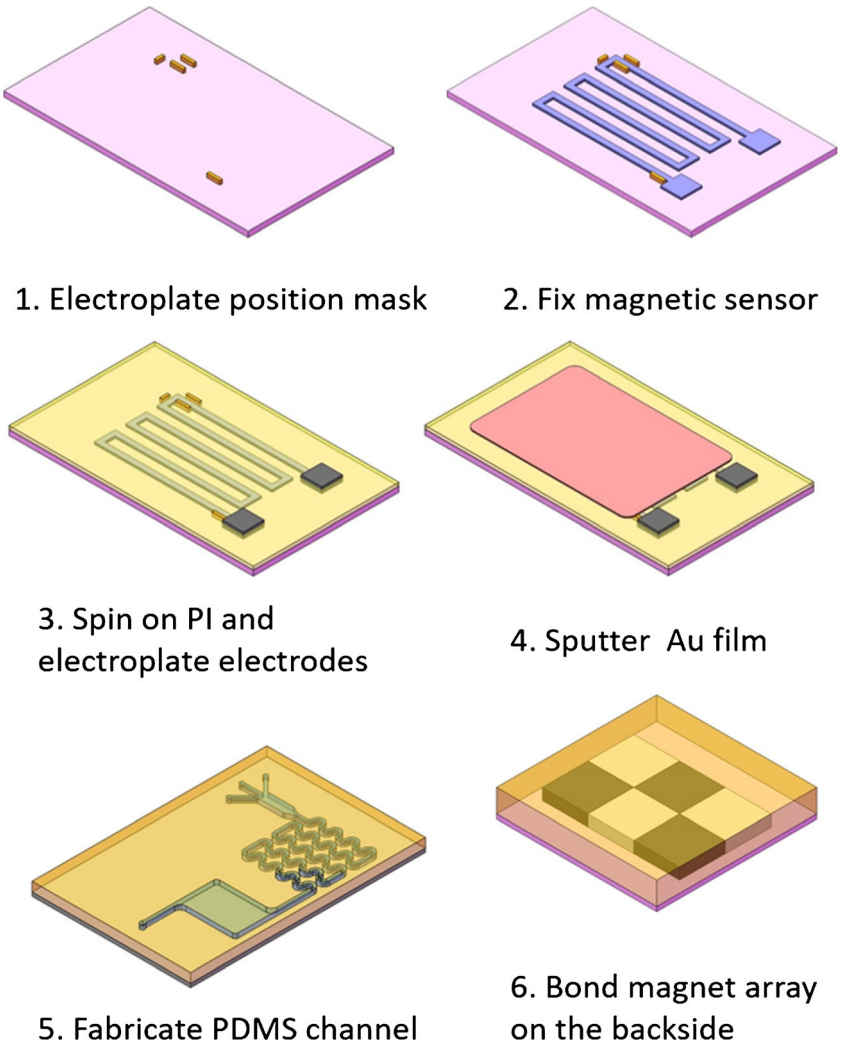

Fig. 3 Fabrication procedure of the integrated magnetic microfluidic chip

substrate. After thermal coagulation in an oven at 80°C for 30 min, PDMS structure was peeled off from the mold and cut to a size (Step 5). The picture of the microfluidics (pumping Safranin T into microchannel) is shown in Fig. 4a. In order to seal microchannel to the substrate, a thin PDMS film was spin-coated (spin speed of 5000 rpm for 30 s) on the biomarker detecting system and coagulated in an oven at 80°C for 30 min. PDMS film covering Au film was removed and other space was retained to reinforce the interaction between microchannel and biomarker detecting system. The PDMS microchannel was bonded to the device above after oxygen plasma treatment.

For PDMS has well bonding strength with glass substrate, magnet array was fixed into PDMS and bonded on the reverse side of glass substrate (with substrate thickness, h = 1mm). The distance and position between magnet and magnetic ribbon can be changed via adjusting the thickness and bonding space of PDMS film (Step 6).

Microfluidic sandwich immunoassays

The processes of microfluidic sandwich immunoassay are shown in Fig. 5. Double antibody sandwich immunoassay and streptavidin-biotin binding assay are used for capturing and labeling PSA. Four major steps are employed in microfluidic sandwich immunoassay:

1. Preprocess Au film to form self-assemble monolayer: Au film was preprocessed before bonding the microchannel to biomarker detecting system. The Au film on biomarker detecting system was ultrasonic cleaned by 1 M NaOH, 1 M HCl, alcohol and deionized water, respectively. To form a self-assemble monolayer on the surface of Au biomarker detecting film, thiols was adsorbed onto the surface of Au film by incubating in 30 mM MPA solution at room temperature for 3 h. The Au film was then flushed with ethanol and deionized water. The biomarker detection system was treated with a solution of 0.2 M EDC and 0.05 M NHS for 40 min at room temperature for activation. Then the activated film was washed with PBS (saline) and dried in air.
2. Immobilization of PSA antibody: Before microfluidic process, PSA antibody was labeled with streptavidin-functionalized IMB. The detail processes are as follows: First, streptavidin-functionalized immunomagnetic beads IMBs were diluted with PBS to obtain the concentration of 100 $\mu g \cdot mL^{-1}$. Biotinylated PSA antibody was diluted with PBS to obtain the concentration of 1 $mg \cdot mL^{-1}$. 20 μL IMB was mixed with 20 μL PSA antibody and incubated at 37°C in thermostatic water bath for 40 min. Five times of magnetic separation were carried out using DynaMag™-Spin Magnet to remove excess biotinylated antibody and solution. Finally, 100 μL immobilized PSA antibody solution was extracted and reserved at 4°C.
3. Immobilization PSA antibodies onto Au film and blocking: After bonding the microchannel with biomarker detecting system, 12 μL PSA antibody solution with a concentration of $1mg \cdot mL^{-1}$ was pumped into the reactive chamber using Syringe pump and incubated at 37°C for 1 h. Au film was washed by pumping PBS (including 1% BSA and 0.05% Tween 20) into reactive chamber. Next, to block the nonspecific adsorption sites, 12 μL BSA solution (including 1% BSA) was pumped into the chamber and incubated at 4°C for 2 h. Unreacted BSA was washed by phosphate buffered saline (PBS).
4. Immunoassay in microfluidics: In order to implement immunological reaction in microfluidics, the immunoreaction platform contains incubation chamber to conjugate

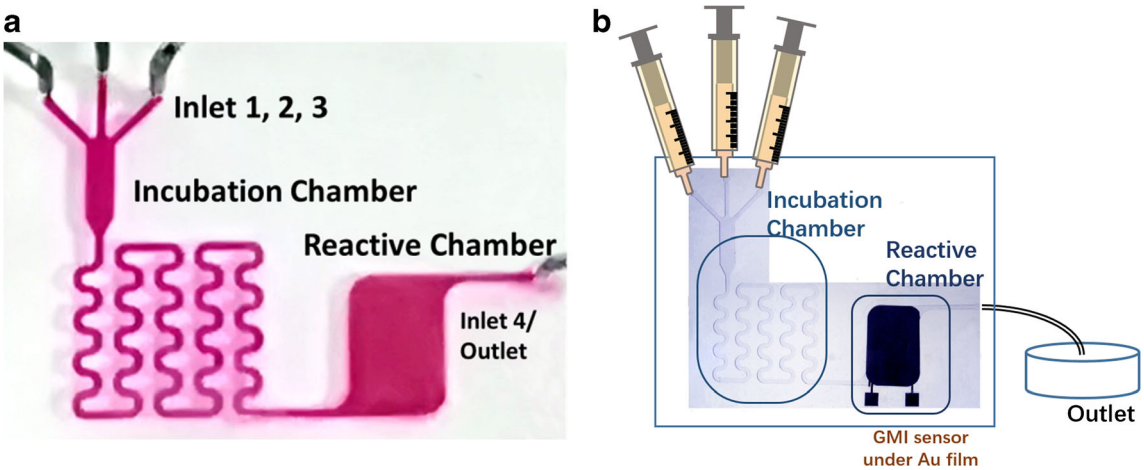

Fig. 4 **a** The picture of the microfluidic (pumping Safranin T into microchannel). **b** Micrographs and immunodetection method of integrated magnetic microfluidic chip

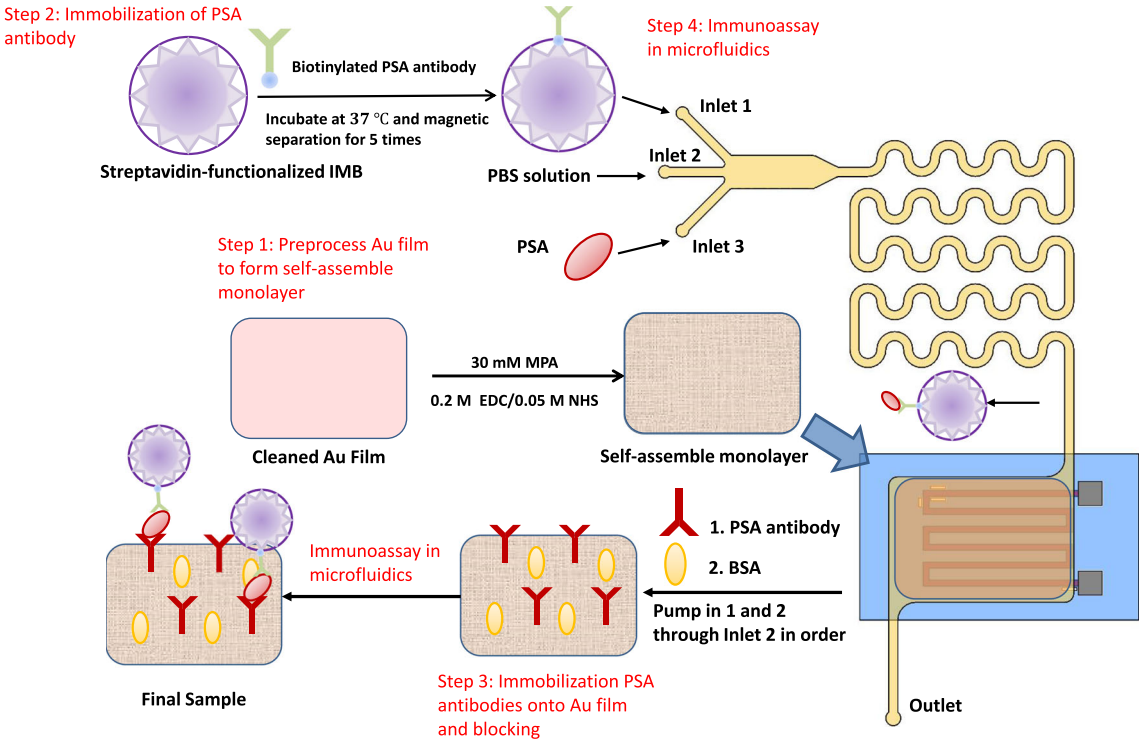

Fig. 5 The processes of microfluidic sandwich immunoassay

PSA with immobilized PSA antibody, and reactive chamber to trap IMB then capturing PSA.

a) Conjugate PSA with immobilized PSA antibody in incubation chamber: PSA was diluted with PBS to a series of concentrations ($0.1\ ng \cdot mL^{-1} - 100\ ng \cdot mL^{-1}$). Immobilized PSA antibody solution was pumped into the microchannel from Inlet 1 through Teflon tubing and PSA was pumped into the microchannel from Inlet 3. The temperature of incubation is 37°C and detail parameters such as design of tortuous incubation chamber, flow rate and volume of reactive solutions are discussed in "Characters of microfluidic immunoreaction platform" section.
b) Trap IMB and capture PSA: Conjugated PSA was pumped into reactive chamber and trapped on the surface of Au film due to the magnetic force between IMB and permanent magnet array. PBS was completely pumped into and filled with reaction chamber from Inlet 2 after removing magnet array. The chip was then incubated at room temperature for 1 h and unimmobilized IMB were washed out with PBS. The sample was prepared for the detection experiments. Figure 4b displays the micrographs and immunodetection method of microfluidic immunoassay.

PSA trapping and analytical system

Trapped IMB was employed as magnetic labels of PSA to generate stray magnetic field and cause a disturbance under the magnetization of the external applied DC magnetic field. In biomarker detection system, the basic principle is, by using GMI sensor, detecting the variation of magnetic signal which caused by IMB labeled PSA.

During the experiment, two electrodes of GMI sensor were connected to the Impedance Analyzer. The fundamental of GMI effect is that the AC impedance in soft magnetic materials changes significantly with the variation of external DC magnetic field [25, 26]. The AC current was injected into the GMI sensor with the frequency of $0.1 - 40$ MHz at a constant amplitude of 10 mA. For the maximum transverse GMI ratio is much less than longitudinal GMI ratio in meander-structured GMI sensor [27], external magnetic field of $0 - 80$ Oe was applied in longitudinal direction. Under the external magnetic field magnetization, the direction of stray magnetic field produced by IMB is opposed to the external field. GMI effect was represented by the relative variation of impedance, which is referred to as GMI ratio: GMI ratio $(\%) = \Delta Z / Z_{max} = [Z(H_{ex}) - Z(H_{max})]/Z(H_{max}) \times 100\%$, where $Z(H_{ex})$ is the impedance under external magnetic field H_{ex}, and Z_{max} is the impedance under the maximum external

magnetic field H_{max}. In this way, PSA can be monitored by detecting the change of GMI ratio using GMI sensor.

Results and discussions

Characters of microfluidic immunoreaction platform

It is well known that response time and reaction efficiency are two of the main influence factors in immunoassay. Therefore, decreasing assay time and enhancing reaction efficiency are of great importance for PoC testing. In microfluidic immunoreaction, reactants inside the microchannel have large surface-to-volume ratio. Shorter reaction time and higher reaction efficiency give this platform obvious advantages over traditional GMI sensors. Besides, circuitous channel increases reaction rate and efficiency in immunoassay.

According to our design, the volume of tortuous incubation chamber is approximately 13 μL. To acquire the optimum reaction efficiency, IMB-labeled PSA antibody solution was pumped into the microchannel from Inlet 1 through Teflon tubing at the flow rate of 25 $\mu L \cdot h^{-1}$and PSA was pumped into from Inlet 3 at the rate of 15 $\mu L \cdot h^{-1}$. Therefore, the time of incubation is 19.5 min, which is suitable for conjugating PSA with antibody. Besides, hydrodynamic drag force is far smaller than magnetic force produced by magnetic trapping array when the flow rate is not high enough. In this way, it meets the needs of trapping IMB labeled PSA in microfluidics efficiently. The volume of immobilized PSA antibody solution is 50 μL and the volume of PSA is 30 μL. After immunoreaction in the reactive chamber, some of the unimmobilized IMB which affect test and analysis were remained in the reactive chamber. Phosphate buffered saline was pumped into the reactive chamber from Inlet 2 to wash out unimmobilized IMB.

Property of magnetic sensors

In our work, immunomagnetic beads were detected by GMI sensor to confirm the reliability of the biochip before PSA immunoassay. Then, PSA was detected by integrated magnetic microfluidic chip. During IMB detection, under the magnetization of external DC magnetic field, IMB generated stray magnetic field and caused a field disturbance. This disturbance can be detected utilizing meander-line structure GMI sensor by the variation of GMI ratio. And in PSA immunodetection by magnetic microfluidic chip, trapped IMB were employed as magnetic labels of PSA to cause a field disturbance. The variation of magnetic signal caused by IMB labeled PSA was measured by using GMI sensor.

As mentioned above, each GMI sensor is integrated into the biochip and hard to separate after measurement. To avoid two experiments interfered with each other, two meander-line structured sensors, namely Sensor-1 and Sensor-2, were chosen for capturing IMB and PSA rather than using single sensor for all samples testing. Two GMI sensors were fabricated into same structure and the detail microfabrication process of GMI sensors is provided in "Fabrication of the GMI sensor" section.

The influence of driving AC frequency and the external DC magnetic field intensity on GMI response was evaluated by Impedance Analyzer to determine optimum experiment parameters using Sensor-1. The impedance change of GMI sensor is little after magnetic field intensity reaches above 150 Oe. In this way, 150 Oe is used as the maximum field intensity H_{max} in GMI ratio calculation ($H_{max} = 150$ Oe). Figure 6a shows the frequency dependences of GMI ratio for the magnetic sensor under different magnetic field intensities. To acquire the maximum GMI ratio, which represents the optimum magnetic property in GMI sensor, an external magnetic field intensity of 0 Oe − 80 Oe is applied along longitudinal direction of the meander-structured GMI sensor. Obviously, there is a slight change of impedance under weak external magnetic field (<5 Oe) and impedance decreases with the increase of driving frequency. However, under relatively strong external field (≥10 Oe), as driving frequency increases, GMI ratio increases sharply and decreases slightly. Figure 6b displays the field dependence of GMI ratio with the frequency from 0 MHz to 40 MHz. With the increase of magnetic field intensity, GMI ratio increases sharply before magnetic field reaches saturation and has a small decrease after saturation field. The optimum GMI ratio is acquired around saturation field.

Biomarker detection system for immunomagnetic beads detection

In this GMI sensor, the immunomagnetic beads (IMB) are supposed to be fully magnetized in order to be detected sensitively. The saturation magnetization of Dynabeads® Myone™ streptavidin M-280 is 14 $kA \cdot m^{-1}$, so IMB have not achieved saturation when external magnetic field intensity is not more than 80 Oe. In order to achieve significant magnetic flux density, external field applied on IMB should generate strongest possible stray magnetic field. However, when the intensity of external field is more than 50 Oe, GMI ratio has a tendency to decrease. In this way, the applied external field was 50 Oe in Sensor-1.

Next, the immunomagnetic beads were pumped into microchannel, trapped by permanent magnet in reaction chamber and detected by GMI sensor. Figure 7a displays the SEM characterization of IMB sample. To acquire the GMI ratio at different concentrations, IMB solutions with a series of concentrations (0.1 $\mu g \cdot mL^{-1}$, 1 $\mu g \cdot mL^{-1}$, 10 $\mu g \cdot mL^{-1}$ and 100 $\mu g \cdot mL^{-1}$) were diluted by phosphate buffered saline, respectively. The volume of the IMB solution was 10 μL.

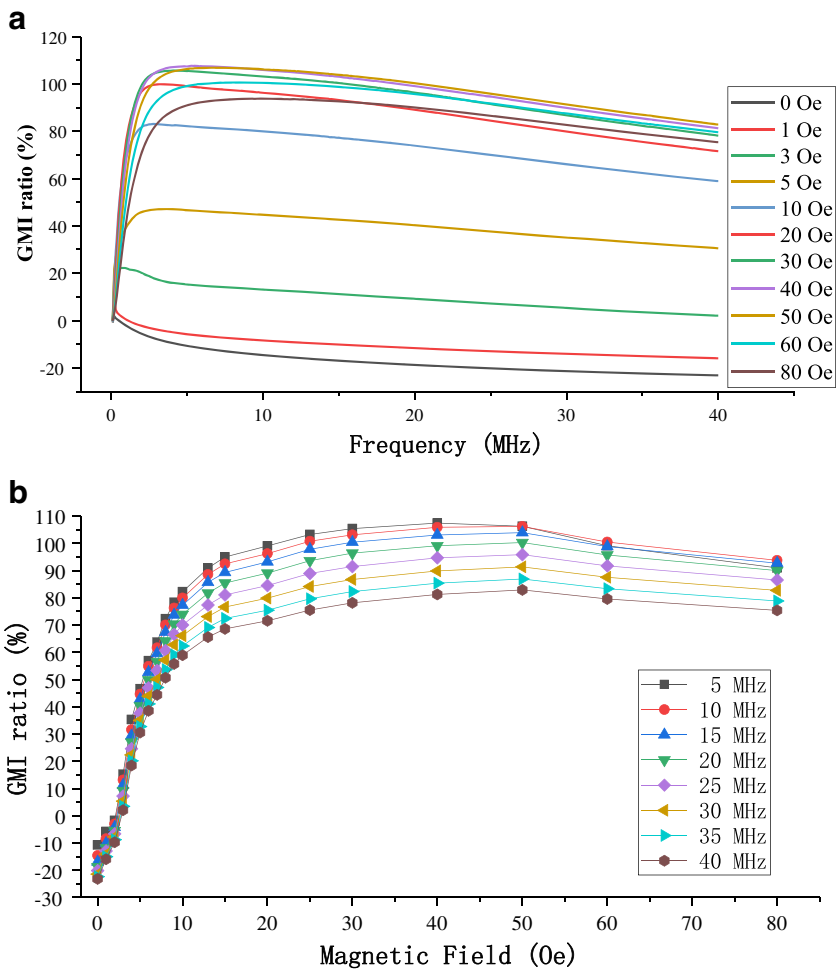

Fig. 6 **a** AC driving frequency dependence of GMI ratio under different magnetic field intensities. **b** DC external magnetic field dependence of GMI ratio at different driving frequencies

Figure 7b shows the frequency dependence of GMI ratio with different IMB concentrations under 50 Oe. At low driving frequency (≤10 MHz), GMI ratio decreases when IMB sample, especially low concentration, was pumped into the reactive chamber. At high driving frequency (≥15 MHz), GMI ratio is considerably increased with the increase of IMB concentration. Two main factors are considered in IMB detection: the stray magnetic field induced by IMB, and magnetic moment rotation at high frequency. The direction of stray magnetic field is opposed to the external magnetic field under external field magnetization, as a result, stray field decreases the response of GMI sensor. However, enhanced magnetic moment rotation can raise transverse permeability, so that GMI property increases. At low frequency, the stray magnetic field induced by IMB decreases GMI ratio when IMB concentration is low and the magnetic moment rotation is not evident. With the increase of IMB concentration, the impact of magnetic rotation is more significant than the impact of stray magnetic field, which increases the response of GMI sensor. When IMB concentration achieves 100 $\mu g \cdot mL^{-1}$, stray magnetic field and magnetic moment rotation nearly offset each other in the effect on GMI property. When driving frequency achieves high frequency, strong rotational magnetization takes the dominant position. The effect of rotational magnetization on IMB with high concentration is more evident than with low concentration. Therefore, GMI ratio is considerably increased with the increase of IMB concentration.

The external field dependence of GMI ratio under the frequency of 23 MHz with different concentrations is shown in Fig. 7c. Under weak magnetic field (≤5 Oe), the difference between IMB samples with different concentrations and control group is small, which is probably attributed to two reasons: the sensitivity of GMI sensor is relatively low and the magnetization of IMB is not large enough to generate strong stray field. Nevertheless, under strong external magnetic field (30 − 60 Oe), the signal difference between IMB samples with different concentrations and control group is evident and this finding may be attributable to the following factors. First, the transverse permeability is increased due to the strong rotational magnetization in the presence of strong external magnetic field [26]. Second, with the increase of external field, IMB tend to be saturation and the stray magnetic field is relative large. From the measurement results, the signal difference between IMB

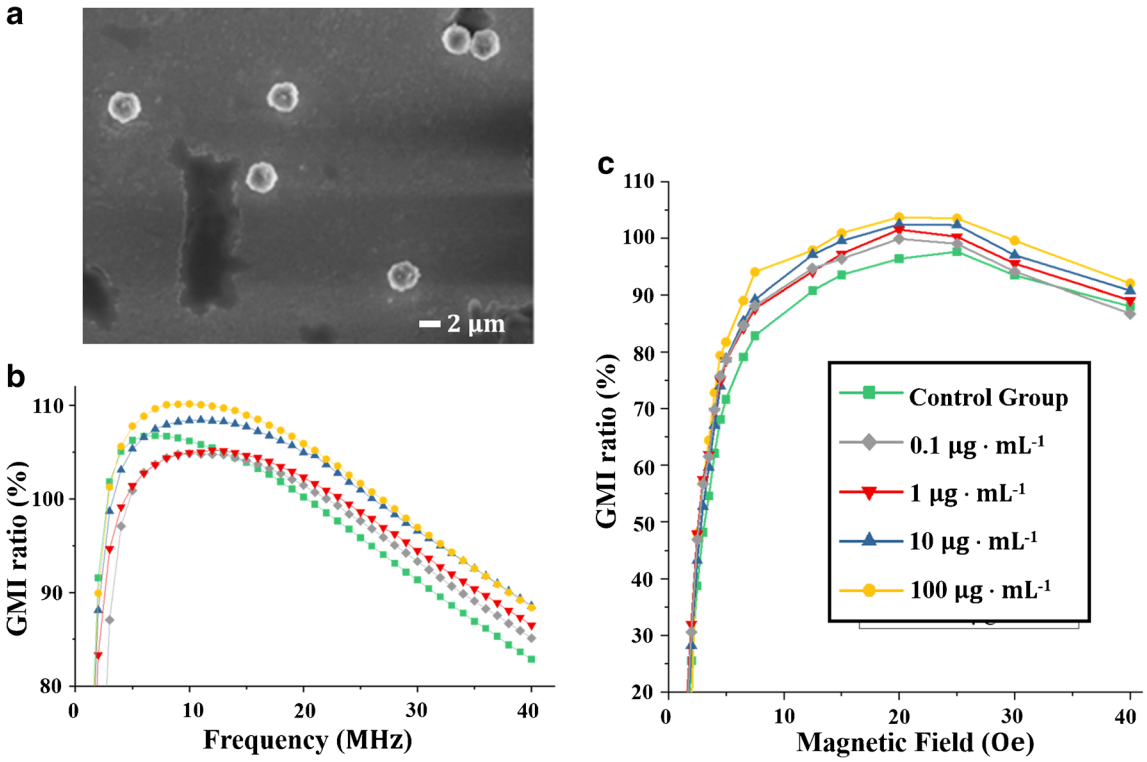

Fig. 7 **a** The SEM characterization of immunomagnetic beads (IMB) sample. **b** Frequency dependence of GMI ratio with different IMB concentrations under 50 Oe. **c** External field dependence of GMI ratio under the frequency of 23 MHz with a series of IMB concentrations

sample and control group is obvious around saturation magnetic field. Furthermore, GMI ratio increases with the increase of IMB concentration. The sensitivity of GMI sensor is ultrahigh and a minimum detectable concentration of 0.1 $\mu g \cdot mL^{-1}$ has been achieved. Besides, the linear fitting result of GMI ratio and IMB concentration by performing 5 independent measurements is shown in Fig. 8. The fitting curve is $Y = 1.92X + 100.24$, in which X presents the concentration and Y presents GMI ratio. Hence, it is expected to detect IMB in biomarker detection system.

PSA detection by integrated magnetic microfluidic chip

As mentioned above, immunodetection of PSA sample is of significance for PCa detection. Five test samples with PSA concentration of 0 $ng \cdot mL^{-1}$, 0.1 $ng \cdot mL^{-1}$, 1 $ng \cdot mL^{-1}$, 5 $ng \cdot mL^{-1}$ and 20 $ng \cdot mL^{-1}$ were prepared respectively and Sensor-2 was chosen for PSA detection. Similar to the measurement in Sensor-1, the optimum parameters were evaluated in Sensor-2. The optimum driving AC frequency is 35 MHz and the applied external magnetic field is 20 Oe. Samples were pumped into biochip and their impedances were detected by Impedance Analyzer in turn. Figure 9a displays the external field dependence of GMI ratio at the frequency of 35 MHz with a series of PSA concentrations, especially under the external field from 5 Oe to 50 Oe. And Fig. 9b shows SEM characterization of IMB labeled PSA sample. GMI ratio is overall increased due to the increase of PSA sample concentration because the concentration of PSA bonded IMB raises. A concentration of 0.1 $ng \cdot mL^{-1}$ was successfully detected by GMI sensor, which can be used for further quantitative analysis. The linear fitting result of GMI ratio and PSA concentration by performing 5 independent measurements is shown in Fig. 10. The fitting curve is $Y = 0.80X + 76.16$, in which X presents PSA concentration and Y presents GMI ratio. A relative standard deviation (RSD) of 0.25% was obtained on 1 $ng \cdot mL^{-1}$,

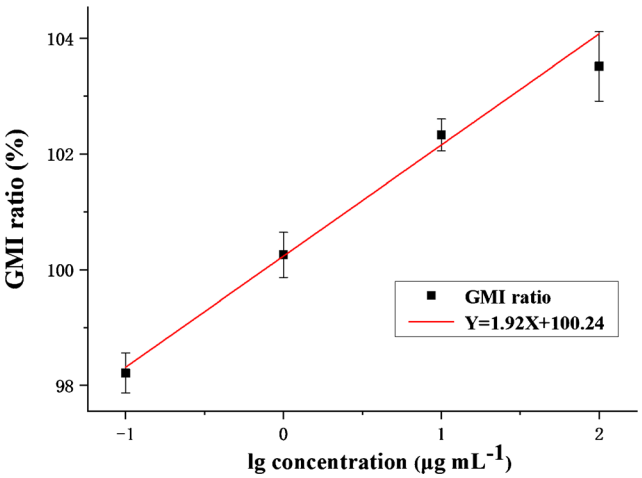

Fig. 8 The linear fitting result of GMI ratio and IMB concentration

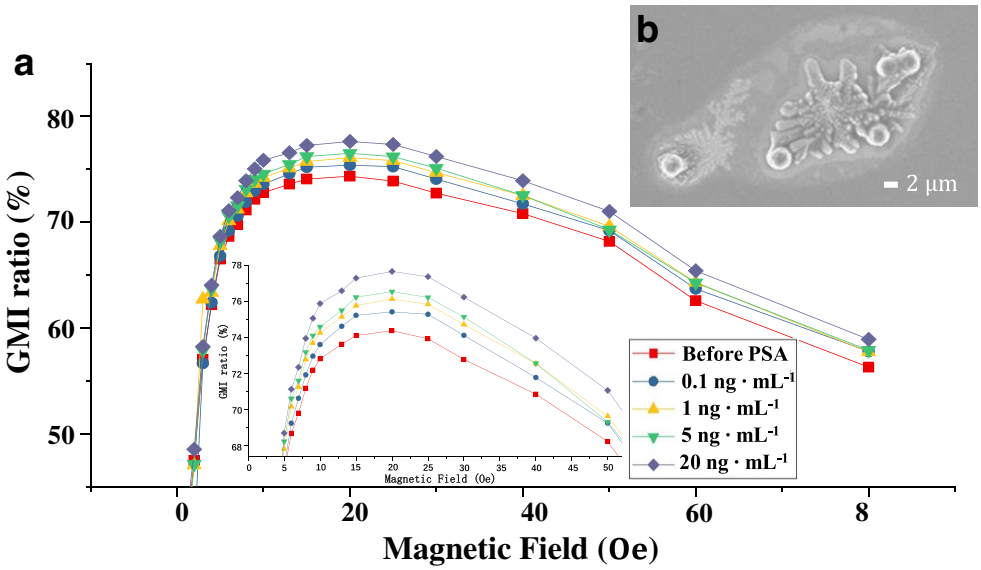

Fig. 9 **a** External field dependence of GMI ratio at the frequency of 35 MHz with different PSA concentrations. **b** SEM characterization of IMB labeled PSA sample

which indicated an acceptable reproducibility in this chip. Besides, according to the previous works in our group [14], GMI biosensor system shows excellent stability after storage in a refrigerator at 4°C for 30 days (the GMI biosensor retained about 98.93% of its initial response).

The specificity of this integrated chip for PSA immunodetection was tested via an interference experiment. The specificity investigation of the integrated magnetic microfluidic chip for PSA detection is shown in Fig. 11. When immunodetection with interfering agents in interference experiment, such as carcino-embryonic antigen (CEA) and alpha fetoprotein (AFP), no significant difference was found in comparison with the blank control. And the difference between free PSA and blank control without immunodetection is not obvious.

In comparison with traditional biomarker detecting methods using magnetic sensors [14, 28, 29], there are four main advantages in integrated magnetic microfluidic chip: First, this chip can avoid complex steps and complicated operations in immunoassay. Second, the surface-to-volume ratio is increased resulting in reducing assay time and enhancing reaction efficiency because the immunoassay is reacted inside the microchannel. Third, the distance between IMB trapping system and GMI sensor in integrated magnetic microfluidic chip is shorter than the distance by separated detection [29]. As a result, stray magnetic field induced by IMB is stronger in integrated chip. This can, in turn, increase the detection sensitivity to biomarkers. Forth, the position relationship between immunoreaction platform and magnetic sensor is accurate, which avoids error in magnetic signal testing. Besides, in comparison with dropwise adding PSA on the substrate, PSA is distributed relatively in order in microfluidic chip

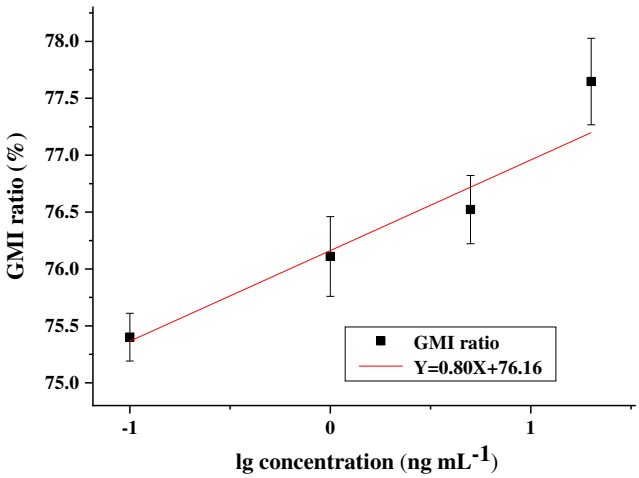

Fig. 10 The linear fitting result of GMI ratio and PSA concentration

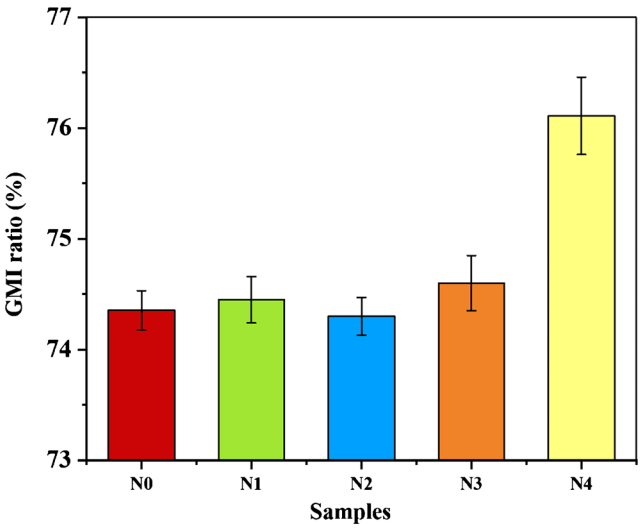

Fig. 11 Specificity investigation of the integrated magnetic microfluidic chip for PSA detection: (N0) blank control, (N1) CEA with the concentration of 1 ng · mL^{-1}, (N2) AFP with the concentration of 1 ng · mL^{-1}, (N3) free PSA with the concentration of 1 ng · mL^{-1}, (N4) PSA labeled IMB with the concentration of 1 ng · mL^{-1}

Table 1 Comparison of different methods for PSA immunodetection

Methods/materials	Detection technique	Analytical range	Detection limit	Detection time	Advantages	Ref.
3D open-structured PtCu nanoframes	Electrochemical immunosensor	0.01–100.0 ng · mL^{-1}	0.003 ng · mL^{-1}	1 h 30 min	Wide linear range, improved reproducibility, selectivity and stability	[29]
CdTe quantum dots	Fluorescence sensor	1.0–40 ng · mL^{-1}	0.4 ng · mL^{-1}	84 min	Simultaneous determination of various kinds of substances on a single chip	[30]
Catalytic effect of ferrocenecarboxylate	Cathodic electro-chemiluminescence	0.005–5 ng · mL^{-1}	0.0017 ng · mL^{-1}	More than 12 h	Ultrasensitive and low detection limit	[31]
AuNPs@GMCs	Electrochemical aptasensor	0.25–200 ng · mL^{-1}	0.25 ng · mL^{-1}	More than 3 h 10 min	High specificity, good stability and repeatability	[32]
Apt/rGO-TiO2(200)/GCE	Electrochemical aptasensor	0.003–1000 ng · mL^{-1}	0.001 ng · mL^{-1}	45 min	High sensitivity, selectivity, and stability	[33]
scAb conjugated to MPs	Magneto-immunosensor	0.5–10 ng · mL^{-1}	0.5 ng · mL^{-1}	More than 1 h 20 min	Low-cost onsite in medical practitioners' surgeries	[34]
H-Gr/PdNP-DNA-Biotin-SA aptasensor	Differential pulse voltammetry	0.025–204.8 ng · mL^{-1}	0.008 ng · mL^{-1}	60 min	Broad linearity, relatively low detection limit	[35]
Co-based GMI sensor	Magnetic microfluidic chip	0.1–20 ng · mL^{-1}	0.1 ng · mL^{-1}	Less than 40 min	Rapid detection and reduction of test steps	Here

due to the magnetic force between IMB and permanent magnet array. Thus, experiment error resulted from IMB clutter distribution is decreased.

The comparison of integrated magnetic microfluidic chip and different methods recently reported for PSA immunodetection is shown in Table 1. Integrated magnetic microfluidic chip provides a relatively effective PSA detecting performance. In comparison to other methods in PSA immunodetection [30–36], this chip does not have the lowest detection limits. However, by using an integrated magnetic microfluidic chip, IMB labeled PSA manipulation, immunoreaction and detection are integrated in one analysis platform. This chip can be adopted to single-step test when serum samples or PBS solutions contain PSA. Specifically, the response time of the biomarker detecting system is less than 5 s. The entire PSA immunodetection period, including PSA samples immunoassay procedures and detection steps, can be accomplished in less than 40 min by using an integrated microfluidic chip. This chip shows the advantages of rapid detection and reduction of test steps. In addition, our proposed chip is convenient to be manipulate, can be miniaturized, and involves no requirement for a lab. On account of these advantages, our integrated magnetic microfluidic chip meets the requirement of clinical PoC diagnostics.

However, to many biochips based immuno-capture based assays [37], there are some challenges in real sample detection, such as repeatability and reusability. The linear fitting of GMI ratio and PSA concentration is not complete, especially when the concentration is different a little. In order to achieve better linear fitting and detection limit, we focus on improving performance of GMI sensor and the efficiency of immunoreaction. In addition, the magnetic property of each GMI sensor in integrated magnetic system is not same due to microfabrication technology limitation. We are carrying on some ways to solve it, such as using laser cutting instead of chemical etching during meander-line structure GMI sensor fabrication and sputtering Au on polyimide film sticky tape by lift-off technology which can be removed conveniently after immunoreaction.

Conclusion

This paper introduce an integrated magnetic microfluidic chip based on using GMI sensor to detect PSA rapidly. The results clearly demonstrate that this integrated chip has potential applications in the field of biomarkers manipulation and detection, and is a promising candidate for the future PoC diagnostics. This integrated magnetic microfluidic chip reduces complex steps, avoids complicated operations and decreases assay time. Besides, this chip enhances immunoreaction efficiency and decreases the experiment error. The sensitivity of integrated chip can be further enhanced by developing microfabrication technology to increase repeatability, employing high performance magnetic material to improve

GMI sensor sensitivity and enhancing the efficiency of immunoreaction during immunodetection. In future study, we will focus on enhancing the sensitivity of integrated magnetic microfluidic chip and expanding the integrated system to detect biomarkers in real samples.

Acknowledgements This work is supported by The National Natural Science Foundation of China (No.61273065), National Science and Technology Support Program (2012BAK08B05), Support fund of Shanghai Jiao Tong University (AgriX2015005), Support fund of Joint research center for advanced aerospace technology of Shanghai Academy of Spaceflight Technology-Shanghai Jiao Tong University (USCAST2015-2), Support fund of aerospace technology (15GFZ-JJ02-05), the Analytical and Testing Center in Shanghai Jiao Tong University, the Center for Advanced Electronic Materials and Devices in Shanghai Jiao Tong University.

Compliance with ethical standards The author(s) declare that they have no competing interests.

References

1. Barbosa AI, Castanheira AP, Edwards AD, Reis NM (2014) A lab-in-a-briefcase for rapid prostate specific antigen (PSA) screening from whole blood. Lab Chip 14:2918–2928
2. Damborska D, Bertok T, Dosekova E, Holazova A, Lorencova L, Kasak P, Tkac J (2017) Nanomaterial-based biosensors for detection of prostate specific antigen. Microchim Acta 184:3049–3067
3. Yang Z, Hordern BK, Goggins S, Frost CG, Estrela P (2015) A novel immobilization strategy for electrochemical detection of cancer biomarkers: DNA-directed immobilization of aptamer sensors for sensitive detection of prostate specific antigens. Analyst 140: 2628–2633
4. Matsumoto K, Konishi N, Hiasa Y, Kimura E, Takahashi Y, Shinohara K, Samori T (1999) A highly sensitive enzyme-linked immunoassay for serum free prostate specific antigen (f-PSA). Clin Chim Acta 281:57–69
5. Liu Y (2008) Electrochemical detection of prostate-specific antigen based on gold colloids/alumina derived sol-gel film. Thin Solid Films 516:1803–1808
6. Ito K, Nishimura W, Maeda M, Gomi K, Inouye S, Arakawa H (2007) Highly sensitive and rapid tandem bioluminescent immunoassay using aequorin labeled Fab fragment and biotinylated firefly luciferase. Anal Chim Acta 588:245–251
7. Baselt DR, Lee GU, Natesan M, Metzger SW, Sheehan PE, Colton RJ (1998) A biosensor based on magnetoresistance technology. Biosens Bioelectron 13:731–739
8. Rife JC, Miller MM, Sheehan PE, Tamanaha CR, Tondra M, Whitman LJ (2003) Design and performance of GMR sensors for the detection of magnetic microbeads in biosensors. Sens Actuators A Phys 107:209–218
9. Besse PA, Boero G, Demierre M, Pott V, Popovic R (2002) Detection of a single magnetic microbead using a miniaturized silicon hall sensor. Appl Phys Lett 80:4199–4201
10. Lei C, Wang R, Zhou Y, Zhou Z (2009) MEMS micro fluxgate sensors with mutual vertical excitation coils and detection coils. Microsyst Technol 15:969–972
11. Mohri K, Bushida K, Noda M, Yoshida H, Panina LV, Uchiyama T (1995) Magneto-Impedance Element. IEEE Trans Magn 31:2455–2460
12. Wang T, Zhou Y, Lei C, Luo J, Xie S, Pu H (2017) Magnetic impedance biosensor: a review. Biosens Bioelectron 90:418–435
13. Guo L, Zhi S, Sun X, Lei C, Zhou Y (2017) Ultrasensitive detection of bioanalytes based on signal amplification of coil-integrated giant magnetoimpedance biosystems. Sens Actuators B Chem 247:1–10
14. Yang Z, Lei C, Zhou Y, Liu Y, Sun X (2015) A GMI biochip platform based on Co-based amorphous ribbon for the detection of magnetic Dynabeads. Anal Methods 7:6883–6889
15. Wang T, Zhou Y, Lei C, Lei J, Yang Z (2013) Development of an ingenious method for determination of Dynabeads protein A based on a giant magnetoimpedance sensor. Sens Actuators B Chem 186: 727–733
16. Sun X, Feng Z, Zhi S, Lei C, Zhang D, Zhou Y (2017) An integrated microfluidic system using a micro-fluxgate and micro spiral coil for magnetic microbeads trapping and detecting. Sci Rep 7:12967–12974
17. Moon S, Keles HO, Ozcan A, Khademhosseini A, Haeggstrom E, Kuritzkes D, Demirci U (2009) Integrating microfluidics and lensless imaging for point-of-care testing. Biosens Bioelectron 24: 3208–3214
18. Wang T, Yang Z, Lei C, Lei J, Zhou Y (2014) An integrated giant magnetoimpedance biosensor for detection of biomarker. Biosens Bioelectron 58:338–344
19. Chen L, Bao C, Yang H, Li D, Lei C, Wang T, Hu H, He M, Zhou Y, Cui D (2011) A prototype of giant magnetoimpedance-based biosensing system for targeted detection of gastric cancer cells. Biosens Bioelectron 26:3246–3253
20. Lin CC, Wang JH, Wu HW, Lee GB (2010) Microfluidic immunoassays. J Lab Autom 15:253–274
21. He H, Yuan Y, Wang W, Chiou NR, Epstein AJ, Lee LJ (2009) Design and testing of a microfluidic biochip for cytokine enzyme-linked immunosorbent assay. Biomicrofluidics 3:022401
22. Zborowski M, Fuh CB, Green R, Sun L, Chalmers JJ (1995) Analytical magnetapheresis of ferritin-labeled lymphocytes. Anal Chem 67:3702–3712
23. Chen L, Zhou Y, Lei C, Zhou Z (2010) Giant magnetoimpedance effect and voltage response in meander shape Co-based ribbon. Appl Phys A Mater Sci Process 98:861–865
24. Panina LV, Mohri K (1994) Magneto-impedance effect in amorphous wires. Appl Phys Lett 65:1189–1191
25. Panina LV, Mohri K, Uchiyama T, Noda M (1995) Giant magneto-impedance in Co-rich amorphous wires and films. IEEE Trans Magn 31:1249–1260
26. Chen L, Zhou Y, Lei C, Zhou Z, Ding W (2009) Effect of meander structure and line width on GMI effect in micro-patterned Co-based ribbon. J Phys D Appl Phys 42:145005
27. Sun X, Lei C, Guo L, Zhou Y (2016) Sandwich immunoassay for the prostate specific antigen using a micro-fluxgate and magnetic bead labels. Microchim Acta 183:2385–2393
28. Wang T, Guo L, Lei C, Zhou Y (2015) Ultrasensitive determination of carcinoembryonic antigens using a magnetoimpedance immunosensor. RSC Adv 5:51330–51336
29. Chen Y, Yuan PX, Wang AJ, Luo X, Xue Y, Zhang L, Feng JJ (2019) A novel electrochemical immunosensor for highly sensitive detection of prostate-specific antigen using 3D open-structured PtCu nanoframes for signal amplification. Biosens Bioelectron 126:187–192
30. Chen Y, Guo X, Liu W, Zhang L (2019) Paper-based fluorometric immunodevice with quantum-dot labeled antibodies for simultaneous detection of carcinoembryonic antigen and prostate specific antigen. Microchim Acta 186:112
31. Zhang F, Mao L, Zhu M (2014) Ultrasensitive immunoassay for free prostate-specific antigen based on ferrocenecarboxylate enhanced cathodic electrochemiluminescence of peroxydisulfate. Microchim Acta 181:1285–1291
32. Liu B, Lu L, Hua E, Jiang S, Xie G (2012) Detection of the human prostate-specific antigen using an aptasensor with gold

nanoparticles encapsulated by graphitized mesoporous carbon. Microchim Acta 178:163–170
33. Karimipour M, Heydari-Bafrooei E, Sanjari M, Johansson MB, Molaei M (2019) A glassy carbon electrode modified with TiO_2(200)-rGO hybrid nanosheets for aptamer based impedimetric determination of the prostate specific antigen. Microchim Acta 186: 33
34. Zapatero-Rodríguez J, Liébana S, Sharma S, Gilgunn S, Drago GA, O'Kennedy R (2018) Detection of free prostate-specific antigen using a novel single-chain antibody (scAb)-based magneto-immunosensor. BioNanoSci 8:680–689
35. Zhang G, Liu Z, Fan L, Guo Y (2018) Electrochemical prostate specific antigen aptasensor based on hemin functionalized graphene-conjugated palladium nanocomposites. Microchim Acta 185:159
36. Issadore D, Park YI, Shao H, Min C, Lee K, Liong M, Weissleder R, Lee H (2014) Magnetic sensing technology for molecular analyses. Lab Chip 14:2385–2397
37. Wiese R, Belosludtsev Y, Powdrill T, Thompson P, Hogan M (2001) Simultaneous Multianalyte ELISA performed on a microarray platform. Clin Chem 47:1451–1457